Journal of Intensive Medicine 3 (2023) 345–351

Contents lists available at ScienceDirect

Journal of Intensive Medicine

journal homepage: www.elsevier.com/locate/jointm

Original Article

Intestinal microbiota dysbiosis and liver metabolomic changes during brain death

Ruolin Tao[1,2], Wenzhi Guo[1,2], Tao Li[3], Yong Wang[2,4,*], Panliang Wang[2,5,*]

[1] Department of Hepatobiliary and Pancreatic Surgery, The First Affiliated Hospital of Zhengzhou University, Zhengzhou 450052, Henan, China
[2] Henan Key Laboratory for Digestive Organ Transplantation, Department of Hepatobiliary and Pancreatic Surgery, The First Affiliated Hospital of Zhengzhou University, Zhengzhou 450052, Henan, China
[3] Department of Biliary Surgery, Nanyang Central Hospital, Nanyang 473009, Henan, China
[4] Department of Anesthesiology, The First Affiliated Hospital of Zhengzhou University, Zhengzhou 450052, Henan, China
[5] Department of Breast Surgery, The First Affiliated Hospital of Zhengzhou University, Zhengzhou 450052, Henan, China

ARTICLE INFO

Keywords:
Brain death
Liver graft
Microbiota
Metabonomic

ABSTRACT

Background: Whether a causative link exists between brain death (BD) and intestinal microbiota dysbiosis is unclear, and the distortion in liver metabolism associated with BD requires further exploration.

Methods: A rat model of BD was constructed and sustained for 9 h (BD group, n=6). The sham group (n=6) underwent the same procedures, but the catheter was inserted into the epidural space without ballooning. Intestinal contents and portal vein plasma were collected for microbiota sequencing and microbial metabolite detection. Liver tissue was resected to investigate metabolic alterations, and the results were compared with those of a sham group.

Results: α-diversity indexes showed that BD did not alter bacterial diversity. Microbiota dysbiosis occurred after 9 h of BD. At the family level, Peptostreptococcaceae and Bacteroidaceae were both decreased in the BD group. At the genus level, *Romboutsia, Bacteroides, Erysipelotrichaceae_UCG_004, Faecalibacterium,* and *Barnesiella* were enriched in the sham group, whereas *Ruminococcaceae_UCG_007, Lachnospiraceae_ND3007_group,* and *Papillibacter* were enriched in the BD group. Short-chain fatty acids, bile acids, and 132 other microbial metabolites remained unchanged in both the intestinal contents and portal vein plasma of the BD group. BD caused alterations in 65 metabolites in the liver, of which, carbohydrates, amino acids, and organic acids accounted for 64.6%. Additionally, 80.0% of the differential metabolites were decreased in the BD group livers. Galactose metabolism was the most significant metabolic pathway in the BD group.

Conclusions: BD resulted in microbiota dysbiosis in rats; however, this dysbiosis did not alter microbial metabolites. Deterioration in liver metabolic function during extended periods of BD may reflect a continuous worsening in energy deficiency.

Introduction

Liver grafts donated from brain-dead patients are the primary sources of liver transplants. Brain death (BD) causes a cascade of catastrophic events involving hemodynamic, hormonal, and inflammatory changes. Whether BD accelerates subsequent graft ischemia-reperfusion injury, thus increasing the risk of complications following transplantation, remains uncertain.[1,2] The liver has substantial resources to withstand harsh turbulence under BD. In comparison, acute kidney injury among patients in an intensive care unit showed an incidence rate of 32.9% and increased the risk of mortality 10-fold.[3] However, functional changes in the liver in response to BD are believed to be more significant than are the morphological changes.[4] Furthermore, whether damages to the graft are caused by BD or by supportive clinical treatment remains unclear. Previous

* Corresponding authors: Panliang Wang, Department of Breast Surgery, The First Affiliated Hospital of Zhengzhou University, Zhengzhou 450052, Henan, China; Yong Wang, Department of Anesthesiology, The First Affiliated Hospital of Zhengzhou University, Zhengzhou 450052, Henan, China.
E-mail addresses: panliang133000@126.com (P. Wang), wangyong200999@126.com (Y. Wang).

https://doi.org/10.1016/j.jointm.2023.02.006
Received 13 November 2022; Received in revised form 17 January 2023; Accepted 25 February 2023. Managing Editor: Jingling Bao.
Available online 10 May 2023

studies on liver grafts have focused on inflammatory changes evoked by BD and have revealed that these inflammatory events are independent of the autonomic storm.[5] Alternatively, the liver is the largest site of "chemical work" in the body, with metabolic activity and involvement in synthesis, decomposition, and detoxification of most substances. Metabolic function is the pathway most affected in grafts following BD.[6] Furthermore, increased anaerobic metabolism accompanied by decreased adenosine triphosphate (ATP) is the most obvious change in graft metabolism during BD.[7] This is caused by an undersupply of oxygen due to hypoperfusion of tissue microcirculation, which is closely associated with mitochondrial impairment.[8] Rat models of BD induced by inflating an intracranial balloon catheter are widely used to study BD because of their flexibility and cost-effectiveness.[9] However, the duration of organ preservation varies from 4 to 10 h under different experimental conditions.[10] Using a rat model of BD sustained for 4 h, Van Erp et al.[11] found that enhanced aerobic metabolism in the liver manifested an increase in hepatic oxygen consumption and a drop in ATP levels, while mitochondrial respiration activity was unaffected. Further characterization of the metabolic changes in this model sustained over a much longer time could expand our knowledge of the metabolic changes that occur in the liver throughout the entire BD process.

BD results in loss of control of the enteric nervous system, which can cause intestinal dysmotility and mucosal damage.[12] The body-wide inflammation caused by BD also results in intestinal damage,[13] which is reciprocally associated with homeostasis in colonization of the gut by resident bacteria. Such microbiota dysbiosis may in turn affect liver function through metabolite transport via the portal vein. Here, we sought to illustrate the microbiota changes that occur during BD in rats to explore another avenue for increasing the preservation of liver grafts.

Methods

Animal model

Male Sprague-Dawley rats weighing 250–280 g were purchased from Hunan SJA Laboratory Animal Company (Wuhan, China) and housed in specific-pathogen-free cages at a constant temperature and humidity, on a 12-h light-dark cycle, with food and water intake *ad libitum*. BD was induced as described previously,[14] and the rats undergoing this procedure (n=6) were termed the BD group. The sham group underwent the same procedures, but the catheter was inserted into the epidural space without ballooning. The Animal Ethics Committee of Zhengzhou University approved the study. The operator (Panliang Wang) is certified to conduct animal experiments.

Sample collection

A midline abdominal incision was made 9 h after inducing BD. The portal vein was dissociated and punctured with a child-sized needle with an attached plastic tube, which was subsequently connected to a heparinized anticoagulant vacuum tube to collect 1 mL of blood. The blood was centrifuged at 2000 r/min for 10 min, then stored at −80 ˚C for future use. Saline (10 mL) was pumped through the needle inserted into the portal vein (5 mL/min), and the postcava was simultaneously incised until the liver became yellowish-gray. The left liver lobe was removed, and liver sections were cut and stored in liquid nitrogen. Intestinal contents from the jejunum to the rectum were collected via curette after opening the intestinal wall, then mixed, homogenized manually, and stored at −80 ˚C. The storage life of the samples was <1 month.

Microbiota sequencing

After thawing, about 150 mg of intestinal contents were weighed, and the bacterial DNA was extracted via the QIAamp Fast DNA Stool Mini Kit (Qiagen, Dusseldorf, Germany) per the manufacturer's protocols. The samples were sequenced, and data were processed as previously described,[15] with a modification of the sequencing region of the bacterial 16S rRNA to the V3–V4 region. The primers used were 338F 5′-ACTCCTACGGGAGGCAGCAG-3′ and 806R 5′-GGACTACHVGGGTWTCTAAT-3′.

Metabolomics

Cold methanol (300 μL) was mixed with 100 μL portal vein plasma and stored at −20 ˚C for 30 min, then centrifuged at 14,000 r/min at 4 ˚C for 10 min. The supernatant was then transferred to an autosampler glass vial and lyophilized. Lyophilized intestinal contents (10 mg) were resuspended in 300 μL NaOH (1 M) and centrifuged at 17,000 r/min at 4 ˚C for 20 min. The supernatant (200 μL) was transferred to an autosampler vial and mixed with 200 μL cold methanol. After the second homogenization and centrifugation, 167 μL of the supernatant was combined with the first supernatant in the sample vial. Liver tissue (50 mg) was added to 10 μL internal standard and 50 μL ice-cold methanol. After homogenization and centrifugation, the supernatant was transferred to an autosampler vial. Prechilled methanol/chloroform (175 μL; 3/1 v/v) was added to the mixture and centrifuged, and the two supernatants were combined and lyophilized under a vacuum. Gas/liquid chromatography (Hewlett Packard, Minneapolis, MN, USA) was used to analyze the three main short-chain fatty acids (SCFAs; acetate, propionate, and butyrate) and 40 bile acids (BAs) in the intestinal contents and portal plasma.[16] Gas chromatography time-of-flight mass spectrometry (GC-TOF-MS) was used for targeted metabolomics of other microbial metabolites of the intestinal contents and portal vein plasma, which included 132 reference compounds.[17] GC-TOF-MS was also used for untargeted metabolomics of the liver samples.[18]

Statistical analysis

Descriptive data are expressed as the mean ± standard deviation or number (percentage). Univariate statistical analysis was performed via the Mann-Whitney U test using SPSS (version 17.0, IBM Corp., Armonk, NY, USA) because most of the data did not comply with a normal distribution. Sequencing data of the microbiota were uploaded and analyzed automatically on the free online platform, Majorbio Cloud Platform (www.majorbio.com). These data mainly included indexes to evaluate bacterial diversity, principal component analysis (PCA), and linear discriminant analysis (LDA). Raw data generated via mass spectroscopy were processed using XploreMET

software (Metabo-Profile, Shanghai, China), which integrates one of the largest metabolite databases, *JiaLib*™. Two statistical analyses were performed using R Studio (http://cran.r-project.org/): (1) multivariate statistical analyses, including PCA, partial least squares discriminant analysis (PLS-DA), and orthogonal partial least squares discriminant analysis (OPLS-DA) and (2) univariate statistical analyses, including Student's *t*-test, the Mann-Whitney *U* test, and analysis of variance. Metabolic pathway enrichment analysis (MPEA) was used to identify the Kyoto Encyclopedia of Genes and Genomes (KEGG) coordinate pathways using metabolite data. P <0.05 was considered statistically significant.

Results

Bacterial diversity and composition evaluation

The Chao1, Sobs, and Shannon indexes of α-diversity were calculated for both the sham and BD groups. Measurements of bacterial richness (estimated via the Chao1 and Sobs indexes) and microbiota diversity (evaluated via the Shannon index) did not differ between the two groups (Table 1). We used PCA to determine the differences in bacterial composition between the groups. The BD-group samples were clustered at a distance from those of the sham group, with the intergroup variation of the microbiota. The principal component explained 48.83% of the data differences, possibly because BD affected the microbiota composition (Figure 1A).

Table 1
Bacterial diversity evaluation of the sham and BD groups.

Index	Sham group (n=6)	BD group (n=6)	P-value
Chao1	358.9 ± 62.2	393.8 ± 41.4	0.6
Sobs	335.3 ± 66.3	343.7 ± 17.7	1.0
Shannon	3.8 ± 0.6	4.0 ± 0.1	1.0

Data are expressed as the mean ± standard deviation and were analyzed via the Mann-Whitney *U* test. Richness and diversity were similar between the two groups.
BD: brain death.

Abundance of differences at the family and genus levels

Up to 98.5% of the bacteria detected in both groups belonged to the phyla Bacteroidetes, Firmicutes, and Proteobacteria, in descending order. From the phylum to order levels, no differences in abundance were observed for any single bacterium between the two groups. However, marginal significance (P =0.05–0.10) was observed starting at the class level. Microbiota dysbiosis occurred after 9 h of BD from the family level. At the family level, differences existed between Peptostreptococcaceae and Bacteroidaceae, both of which were decreased in the BD group. At the genus level, *Romboutsia, Bacteroides, Erysipelotrichaceae_UCG_004, Faecalibacterium,* and *Barnesiella* were enriched in the sham group, whereas *Ruminococcaceae_UCG_007, Lachnospiraceae_ND3007_group,* and *Papillibacter* were enriched in the BD group. Figure 1B shows the differential microorganisms at the family and genus levels according to LDA.

BD did not affect SCFAs, BAs, or other microbial metabolites

We tested the levels of SCFAs, BAs, and other microbial metabolites in the intestinal contents and portal vein plasma. BD did not alter the acetate, propionate, or butyrate levels in the intestinal contents or the portal vein plasma (Figure 2). Among the 40 BA species, 24 were detected in the intestinal contents, and 15 were detected in the portal vein plasma. The absolute values of each BA component did not differ between the groups in either the intestinal contents or portal vein plasma after 9 h (Table 2). None of the 84 other metabolites detected in the intestinal contents or the 55 other metabolites detected in the

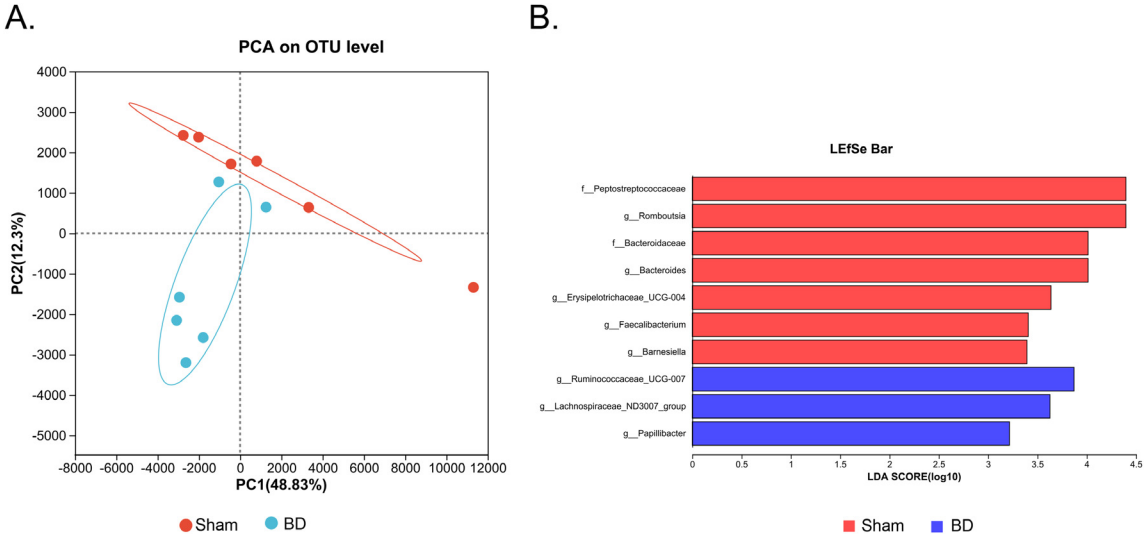

Figure 1. Analysis of microbiota dysbiosis in a rat model 9 h after inducing BD. A: PCA revealed distance between the sample clusters of the BD and sham groups, and the principal component explained 48.83% of the data variation at the X-axis. B: The column bar shows differential microbiotas at the family and genus levels via LDA.
BD: brain death; LDA: linear discriminant analysis; LEfSe: linear discriminant analysis effect size; OTU: operational taxonomic unit; PCA: Principal component analysis.

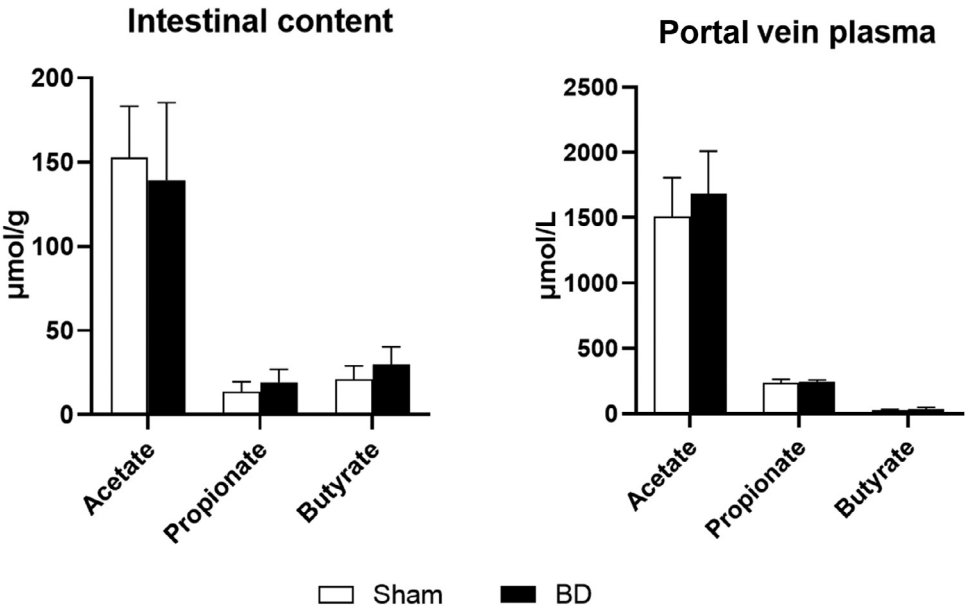

Figure 2. SCFAs levels in a rat model of BD. Acetate, propionate, and butyrate levels were unchanged in the intestinal contents and portal vein plasma after 9 h of BD.
BD: brain death; SCFA: Short-chain fatty acids.

Table 2
BA profiles of the intestinal contents and portal vein plasma.

BA	Intestinal content (μmol/g)		Portal vein plasma (μmol/L)	
	Sham group	BD group	Sham group	BD group
CA	$(4.5 \pm 1.8) \times 10^{-1}$	$(5.1 \pm 1.5) \times 10^{-1}$	85.3 ± 16.8	86.2 ± 9.2
CDCA	$(2 \pm 0.2) \times 10^{-1}$	$(1.9 \pm 0.2) \times 10^{-1}$	4.9 ± 0.7	4.8 ± 0.7
GCA	$(3.8 \pm 0.6) \times 10^{-2}$	$(4 \pm 0.7) \times 10^{-2}$	ND	ND
TCA	1.4 ± 0.3	1.3 ± 0.2	11.4 ± 3.4	12.1 ± 3.0
GCDCA	$(5.6 \pm 0.8) \times 10^{-3}$	$(6.4 \pm 1.1) \times 10^{-3}$	ND	ND
TCDCA	$(6.5 \pm 1.1) \times 10^{-1}$	$(7.3 \pm 1.6) \times 10^{-1}$	1.2 ± 0.2	1.2 ± 0.3
LCA	$(2.0 \pm 0.3) \times 10^{-2}$	$(2.0 \pm 0.3) \times 10^{-2}$	$(6.4 \pm 1.7) \times 10^{-1}$	$(6.3 \pm 1.8) \times 10^{-1}$
HDCA	$(5.0 \pm 1.1) \times 10^{-1}$	$(5.0 \pm 1.1) \times 10^{-1}$	22.9 ± 1.4	22.6 ± 1.3
DCA	$(2.0 \pm 0.2) \times 10^{-1}$	$(2.0 \pm 0.2) \times 10^{-1}$	5.6 ± 0.6	5.5 ± 1.0
UDCA	ND	ND	1.1 ± 0.2	1.1 ± 0.3
GLCA	$(2.6 \pm 2.1) \times 10^{-5}$	$(3.0 \pm 1.6) \times 10^{-5}$	ND	ND
GDCA	$(4.2 \pm 3.3) \times 10^{-3}$	$(3.2 \pm 3.5) \times 10^{-3}$	ND	ND
GUDCA	$(6.9 \pm 1.4) \times 10^{-3}$	$(6.4 \pm 3.2) \times 10^{-3}$	ND	ND
TUDCA	$(7.0 \pm 2.3) \times 10^{-1}$	$(7.0 \pm 1.8) \times 10^{-1}$	$(5.0 \pm 1.2) \times 10^{-1}$	$(4.8 \pm 0.9) \times 10^{-1}$
α-MCA	$(3.3 \pm 0.8) \times 10^{-2}$	$(3.1 \pm 1.1) \times 10^{-2}$	1.8 ± 0.4	1.8 ± 0.3
ω-MCA	$(6.0 \pm 6.7) \times 10^{-3}$	$(7.8 \pm 6.6) \times 10^{-3}$	ND	ND
β-MCA	$(1.1 \pm 0.3) \times 10^{-1}$	$(1.1 \pm 0.2) \times 10^{-1}$	3.0 ± 0.5	3.1 ± 0.3
MDCA	$(8.0 \pm 1.3) \times 10^{-3}$	$(8.6 \pm 2.3) \times 10^{-3}$	ND	ND
TLCA	$(5.5 \pm 2.8) \times 10^{-3}$	$(4.5 \pm 2.7) \times 10^{-3}$	$(4.0 \pm 0.5) \times 10^{-1}$	$(4.0 \pm 1.2) \times 10^{-1}$
THDCA	1.0 ± 0.2	0.9 ± 0.1	ND	ND
TDCA	$(3.1 \pm 0.6) \times 10^{-1}$	$(2.9 \pm 0.6) \times 10^{-1}$	$(9.0 \pm 1.7) \times 10^{-1}$	$(9.1 \pm 2.3) \times 10^{-1}$
Tα-MCA	$(8.1 \pm 2) \times 10^{-1}$	$(7.4 \pm 2.1) \times 10^{-1}$	$(8.2 \pm 1.8) \times 10^{-1}$	$(8.4 \pm 2.4) \times 10^{-1}$
Tβ-MCA	$(2.7 \pm 0.8) \times 10^{-1}$	$(2.8 \pm 0.6) \times 10^{-1}$	1.3 ± 0.1	1.3 ± 0.1
GHDCA	$(5.4 \pm 2.9) \times 10^{-3}$	$(5.0 \pm 2.6) \times 10^{-3}$	ND	ND
MuroCA	$(10.0 \pm 3.7) \times 10^{-2}$	$(10.0 \pm 3.0) \times 10^{-2}$	ND	ND

BA: Bile acid; BD: Brain death; CA: cholate; CDCA: Chenodeoxycholate; DCA: Deoxycholate; GCA: glycocholate; GCDCA: Glycochenodeoxycholate; GDCA: Glycodeoxycholate; GHDCA: G ycohyodeoxycholate; GLCA: G lycolithocholate; GUDCA: G lycoursodeoxycholic acid; HDCA: Hyodeoxycholate; LCA: Lithocholate; MDCA: Murideoxycholate; ND: Not detected, TCA: Taurocholate; TDCA: T aurodeoxycholate; TCDCA: T aurochenodeoxycholate; THDCA: T aurohyodeoxycholate; TLCA: T aurolithocholate; TUDCA: T auroursodeoxycholate; UDCA: Ursodeoxycholate; α-MCA: α-muricholate; β-MCA: β-muricholate; ω-MCA: ω-muricholate; Tα-MCA: Tauro-α-muricholate; Tβ-MCA: Tauro-β-muricholate; MuroCA: Muricholic acid.

portal vein plasma differed between the groups (Supplementary Tables S1 and S2).

Changes in liver metabolism under BD

Overall, 124 metabolites were identified in *JiaLib*^{TM}; 34 metabolic enzymes were detected via KEGG metabolic pathways, and 147 metabolites were unidentified. PCA, PLS-DA, and OPLS-DA were used to reveal the overall metabolic profile similarities and dissimilarities between the groups. First, an unsupervised PCA model demonstrated that each sample could be clearly divided, and no abnormal samples were rejected. Sample clusters were distant between the two groups, although two sham group samples became closer to the BD-group cluster (Supplementary Figure S1A). PLS-DA and OPLS-DA showed more distinct separation (Supplementary Figure S1B, S1C). Permuta-

Table 3
The key metabolic pathways and involved upregulated and downregulated metabolites revealed by MPEA.

Pathway name (BD *vs.* Sham)	*P*. hyper	Up	Down
Galactose metabolism	6.1×10^{-5}*		Galactitol; D-glucose; glycerol; D-galactose; α-lactose; myo-inositol; sorbitol
Neomycin, kanamycin, and gentamicin biosynthesis	1.6×10^{-3}*		D-Glucose; glucose 6-phosphate
Pentose and glucuronate interconversions	5.0×10^{-3}*	D-Ribulose 5-phosphate	D-Xylose; D-glucuronic acid; D-xylitol
Biosynthesis of unsaturated fatty acids	2.4×10^{-2}*		Oleic acid; palmitic acid; linoleic acid; stearic acid
Starch and sucrose metabolism	3.4×10^{-2}*		D-Glucose; D-maltose; glucose 6-phosphate
Glyoxylate and dicarboxylate metabolism	3.4×10^{-2}*		Glycolic acid; L-serine; pyruvic acid; L-glutamine
Ascorbate and aldarate metabolism	4.0×10^{-2}*		D-Glucuronic acid; myoinositol
Phenylalanine metabolism	8.0×10^{-2}†	L-Phenylalanine	Hippuric acid

BD: Brain death; MPEA: Metabolic pathway enrichment analysis.
* $P \leq 0.05$.
† $0.05 < P \leq 0.10$.

tion testing was used to assess the validity of the classification model, and Q2 was −0.204 on the Y-axis, confirming the model's validity (Supplementary Figure S1D).

Metabolic details and related pathway dissimilarities

Differential metabolites were assessed using multivariate statistics with OPLS-DA model values; univariate statistics were assessed using Student's *t*-test or the Mann-Whitney *U* test. Sixty-five metabolites differed between the two groups: 52 were decreased, and 13 were increased in the BD group. Among these 65 differential metabolites, 20 were carbohydrates, 14 were amino acids, and 8 were organic acids, accounted for 64.6% (Supplementary Table S3). Among the decreased metabolites in the BD group, glycerol, sorbitol, allose, D-galactose, and glycerol-3-phosphate (three of which are carbohydrates) showed the largest differences. Among the increased metabolites in the BD group, L-α-aminobutyric acid, 2-hydroxybutyric acid, the D-ribulose-5-phosphate/D-ribose ratio, hypotaurine, and glutaric acid/sarcosine (three of which are amino acids) showed the largest differences. MPEA revealed eight key metabolic pathways (Table 3), with galactose metabolism being the most significant, followed by neomycin, kanamycin and gentamicin biosynthesis, and pentose and glucuronate interconversions. The upregulated and downregulated metabolites are also shown.

Discussion

Most clinical BDs are caused by head trauma, infarction, or hemorrhaging. Studies have revealed that these three forms of brain injury lead to different types of microbiota dysbiosis via different mechanisms.[19] However, the worst form of bodily damage resulting from BD is a harsh physiological process characterized by "catecholamine storms,"[20] which can cause marked changes at the genus level. In the present study, microbiota dysbiosis occurred at the family and genus levels 9 h after BD. Peptostreptococcaceae, which predominates in the ileum, has been positively associated with primary BA production.[21] Bacteroidaceae is the core microbe in the rat cecum and is responsible for producing amino acids, neurotransmitters, and SCFAs, as well as BA biotransformation.[22] The core microbes in the rat colon are Lachnospiraceae and Ruminococcaceae, specifically *Lachnospiraceae_ND3007_group*, which produces butyric acid,[23] and *Ruminococcaceae_UCG-007*, which has been positively correlated with elevated acetate, butyrate, and total SCFA concentrations.[24] *Papillibacter* belongs to *Clostridium* cluster IV and is a butyrate-producing bacterium.[25] *Romboutsia* belongs to Peptostreptococcaceae. *Barnesiella*,[26] *Faecalibacterium*,[27] and *Erysipelotrichaceae_UCG_004*[28] ferment carbohydrates into SCFAs in the colon. The gastrointestinal tract mainly releases noradrenaline via the autonomic nervous system, and intestinal bacteria have receptors that sense variations in host noradrenaline.[19,29] Thus, we speculate that noradrenaline variation may be the main cause of microbiota dysbiosis during BD; however, this requires further research.

Nearly all of the microbial genera that showed changes in response to BD in our model rats were involved in SCFA and/or BA biosynthesis. However, 9 h after inducing BD, measurements of the three main SCFAs and the BA spectrum were unchanged in the intestinal contents and portal vein plasma. We further expanded the search scope to test the production of 132 additional co-metabolites and still found no changes. This may have been because our rat model was difficult to sustain beyond 9 h.[30] Although microbiota dysbiosis occurred, the α-diversity indexes did not significantly differ and few genera were changed, indicating that 9 h was insufficient to yield changes in metabolites. Marginally significant differences began to show at the class level, and changes in more genera might be expected over longer time periods. Further studies using primate models or clinical samples may clarify this.

Our liver metabolomic results showed an overall deterioration in metabolic function, with nearly 80.0% of the differential metabolites showing decreased levels in the liver at 9 h post-BD, the highest proportion of which (30.8%) were carbohydrates. These results differ from the metabolic changes observed at 4 h post-BD. We speculate that the continuous shortage in energy supply was increasingly aggravated over time, consistent with previous findings that mitochondrial dysfunction was the most significant ultrastructural alteration in BD due to impaired hepatic sinusoidal perfusion.[31] This was also confirmed by the increases in toxic and stress-response metabolites in the BD-group livers. These metabolites included L-α-aminobutyric acid, which is toxic[32]; 2-hydroxybutyric acid, which is associated with disrupted mitochondrial energy metabolism and increased oxidative stress[33]; and the D-ribulose-5-phosphate/D-ribose ratio, which is important for maintaining redox homeostasis via the non-oxidative pentose-phosphate pathway.[34] The galactose metabolism pathway is also associated with energy, and the liver is the most important organ in galactose metabolism. Seven metabolites are involved in galactose metabolism, and all were decreased in the BD-group liv-

ers. The most important pathway for using galactose is the Leloir pathway, in which the first step is the conversion of galactose to α-D-galactose from its β-anomer via the action of galactose mutarotase. Deficiency of α-D-galactose leads to restrained glycolysis capacity and less glucose production.[35] Galactose can also be converted to sorbitol, glucose, and myo-inositol via α-galactosidase enzymolysis. Decreases in these three metabolites in the BD-group livers were likely due to α-galactosidase enzymolysis deficiency, which similarly occurs in several malignancies.[18] Other significantly altered pathways in the BD-group livers exhibited metabolic hypofunction caused by decreased metabolites. Glucuronate metabolic disorder weakens detoxification functions[36] and fatty acid and starch metabolism, which are vital for maintaining normal cell organization and biological functions.[37,38] Repeated involvement of glucose and glucose-6-phosphate in three pathways strengthens the core importance of energy metabolism in the liver during BD.

Conclusions

We illustrated the intestinal microbial changes that occur during BD using a rat model. Because of the short timeframe, microbiota alterations at the family and genus levels were restrained, and the genus-level changes were insufficient to induce changes in microbial metabolites. Untargeted metabolomics revealed reduced metabolic functions in rat livers, with two prominent features. First, differential metabolites and pathways were both associated with energy metabolism and second, the liver was extremely deprived of energy under an extended period of BD (9 h). Measures to correct this energy deficiency, particularly that caused by mitochondrial dysfunction, could be valuable to graft protection.

Author Contributions

Conceptualization: Ruo-Lin Tao and Pan-Liang Wang. Methodology: Tao Li, Wen-Zhi Guo. Data curation: Yong Wang. Formal analysis: Tao Li, Wen-Zhi Guo. Writing original draft: Pan-Liang Wang. Writing review & editing: Yong Wang.

Acknowledgments

We acknowledge the support of Dr. Shui-Jun Zhang, Henan Key Laboratory of Digestive Organ Transplantation, The First Affiliated Hospital of Zhengzhou University for the study design. We also thank Traci Raley, MS, ELS, and Michelle Kahmeyer-Gabbe, PhD, both from Liwen Bianji (Edanz) (www.liwenbianji.cn/), for editing drafts of this manuscript.

Funding

This study was supported by the National Natural Science Foundation of China (grant numbers: 81,900,596, 81,671,958).

Ethics Statement

This study was approved by the Animal Ethics Committee of Zhengzhou University.

Conflict of Interest

The authors declare that they have no known competing financial interests or personal relationships that could have appeared to influence the work reported in this paper.

Data Availability

The data sets generated during and/or analyzed during the current study are available from the corresponding author upon reasonable request.

Supplementary Materials

Supplementary material associated with this article can be found, in the online version, at doi:10.1016/j.jointm.2023.02.006.

References

[1] Ritschl PV, Ashraf MI, Oberhuber R, Mellitzer V, Fabritius C, Resch T, et al. Donor brain death leads to differential immune activation in solid organs but does not accelerate ischaemia-reperfusion injury. J Pathol 2016;239(1):84–96. doi:10.1002/path.4704.
[2] Dziodzio T, Biebl M, Pratschke J. Impact of brain death on ischemia/reperfusion injury in liver transplantation. Curr Opin Organ Transplant 2014;19(2):108–14. doi:10.1097/MOT.0000000000000061.
[3] Santos PR, Monteiro DL. Acute kidney injury in an intensive care unit of a general hospital with emergency room specializing in trauma: an observational prospective study. BMC Nephrol 2015;16:30. doi:10.1186/s12882-015-0026-4.
[4] Pratschke J, Neuhaus P, Tullius SG. What can be learned from brain-death models? Transpl Int 2005;18(1):15–21. doi:10.1111/j.1432-2277.2004.00018.x.
[5] Simas R, Ferreira SG, Menegat L, Zanoni FL, Correia CJ, Silva IA, et al. Mesenteric hypoperfusion and inflammation induced by brain death are not affected by inhibition of the autonomic storm in rats. Clinics (Sao Paulo) 2015;70(6):446–52. doi:10.6061/clinics/2015(06)11.
[6] Akhtar MZ, Huang H, Kaisar M, Lo Faro ML, Rebolledo R, Morten K, et al. Using an integrated -omics approach to identify key cellular processes that are disturbed in the kidney after brain death. Am J Transplant 2016;16(5):1421–40. doi:10.1111/ajt.13626.
[7] Novitzky D, Wicomb WN, Cooper DK, Tjaalgard MA. Improved cardiac function following hormonal therapy in brain dead pigs: relevance to organ donation. Cryobiology 1987;24(1):1–10. doi:10.1016/0011-2240(87)90002-2.
[8] Sztark F, Thicoïpé M, Lassié P, Petitjean ME, Dabadie P. Mitochondrial energy metabolism in brain-dead organ donors. Ann Transplant 2000;5(4):41–4.
[9] van Zanden JE, Rebolledo RA, Hoeksma D, Bubberman JM, Burgerhof JG, Breedijk A, et al. Rat donor lung quality deteriorates more after fast than slow brain death induction. PLoS ONE 2020;15(11):e0242827. doi:10.1371/journal.pone.0242827.
[10] Zens TJ, Danobeitia JS, Chlebeck PJ, Zitur LJ, Odorico S, Brunner K, et al. Guidelines for the management of a brain death donor in the rhesus macaque: a translational transplant model. PLoS ONE 2017;12(9):e0182552. doi:10.1371/journal.pone.0182552.
[11] Van Erp AC, Rebolledo RA, Hoeksma D, Jespersen NR, Ottens PJ, Nørregaard R, et al. Organ-specific responses during brain death: increased aerobic metabolism in the liver and anaerobic metabolism with decreased perfusion in the kidneys. Sci Rep 2018;8(1):4405. doi:10.1038/s41598-018-22689-9.
[12] Li L, Gao Y, Lu C, Guo M. Characterization of the intestinal graft in a swine hypotensive after brain death model. Acta Cir Bras 2020;34(11):e201901107. doi:10.1590/s0102-865020190110000007.
[13] Weaver JL, Matheson PJ, Matheson A, Graham V, Harbrecht BG, Downard CD, et al. Direct peritoneal resuscitation reduces intestinal permeability after brain death. J Trauma Acute Care Surg 2018;84(2):265–72. doi:10.1097/TA.0000000000001742.
[14] Chen S, Fang H, Li J, Shi JH, Zhang J, Wen P, et al. Donor brain death leads to a worse ischemia-reperfusion injury and biliary injury after liver transplantation in rats. Transplant Proc 2020;52(1):373–82. doi:10.1016/j.transproceed.2019.10.012.
[15] Wang P, Wang Y, Lu L, Yan W, Tao Y, Zhou K, et al. Alterations in intestinal microbiota relate to intestinal failure-associated liver disease and central line infections. J Pediatr Surg 2017;52(8):1318–26. doi:10.1016/j.jpedsurg.2017.04.020.
[16] Zhou K, Wang J, Xie G, Zhou Y, Yan W, Pan W, et al. Distinct plasma bile acid profiles of biliary atresia and neonatal hepatitis syndrome. J Proteome Res 2015;14(11):4844–50. doi:10.1021/acs.jproteome.5b00676.
[17] Zhao L, Ni Y, Su M, Li H, Dong F, Chen W, et al. High throughput and quantitative measurement of microbial metabolome by gas chromatography/mass spectrometry using automated alkyl chloroformate derivatization. Anal Chem 2017;89(10):5565–77. doi:10.1021/acs.analchem.7b00660.
[18] Shang X, Zhong X, Tian X. Metabolomics of papillary thyroid carcinoma tissues: potential biomarkers for diagnosis and promising targets for therapy. Tumour Biol 2016;37(8):11163–75. doi:10.1007/s13277-016-4996-z.

[19] Houlden A, Goldrick M, Brough D, Vizi ES, Lénárt N, Martinecz B, et al. Brain injury induces specific changes in the caecal microbiota of mice via altered autonomic activity and mucoprotein production. Brain Behav Immun 2016;57:10–20. doi:10.1016/j.bbi.2016.04.003.
[20] Bittner HB, Kendall SW, Chen EP, Van Trigt P. Endocrine changes and metabolic responses in a validated canine brain death model. J Crit Care 1995;10(2):56–63. doi:10.1016/0883-9441(95)90017-9.
[21] Zhang L, Wu W, Lee YK, Xie J, Zhang H. Spatial heterogeneity and co-occurrence of mucosal and luminal microbiome across swine intestinal tract. Front Microbiol 2018;9:48. doi:10.3389/fmicb.2018.00048.
[22] Curtis K, Stewart CJ, Robinson M, Molfese DL, Gosnell SN, Kosten TR, et al. Insular resting state functional connectivity is associated with gut microbiota diversity. Eur J Neurosci 2019;50(3):2446–52. doi:10.1111/ejn.14305.
[23] Zhong S, Ding Y, Wang Y, Zhou G, Guo H, Chen Y, et al. Temperature and humidity index (THI)-induced rumen bacterial community changes in goats. Appl Microbiol Biotechnol 2019;103(7):3193–203. doi:10.1007/s00253-019-09673-7.
[24] Shi Y, Miao ZY, Su JP, Wasser SK. Shift of maternal gut microbiota of tibetan antelope (Pantholops hodgsonii) during the periparturition period. Curr Microbiol 2021;78(2):727–38. doi:10.1007/s00284-020-02339-y.
[25] Zhou Y, Wang Y, Quan M, Zhao H, Jia J. Gut microbiota changes and their correlation with cognitive and neuropsychiatric symptoms in alzheimer's disease. J Alzheimers Dis 2021;81(2):583–95. doi:10.3233/JAD-201497.
[26] Zeng H, Ishaq SL, Liu Z, Bukowski MR. Colonic aberrant crypt formation accompanies an increase of opportunistic pathogenic bacteria in C57BL/6 mice fed a high-fat diet. J Nutr Biochem 2018;54:18–27. doi:10.1016/j.jnutbio.2017.11.001.
[27] Martín R, Miquel S, Chain F, Natividad JM, Jury J, Lu J, et al. Faecalibacterium prausnitzii prevents physiological damages in a chronic low-grade inflammation murine model. BMC Microbiol 2015;15:67. doi:10.1186/s12866-015-0400-1.
[28] Huang X, Dong W, Wang H, Feng Y. Role of acid/alkali-treatment in primary sludge anaerobic fermentation: insights into microbial community structure, functional shifts and metabolic output by high-throughput sequencing. Bioresour Technol 2018;249:943–52. doi:10.1016/j.biortech.2017.10.104.
[29] Karavolos MH, Winzer K, Williams P, Khan CM. Pathogen espionage: multiple bacterial adrenergic sensors eavesdrop on host communication systems. Mol Microbiol 2013;87(3):455–65. doi:10.1111/mmi.12110.
[30] Zhang S, Cao S, Wang T, Yan B, Lu Y, Zhao Y. Modified brain death model for rats. Exp Clin Transplant 2014;12(5):469–73. doi:10.6002/ect.2013.0229.
[31] Yamagami K, Hutter J, Yamamoto Y, Schauer RJ, Enders G, Leiderer R, et al. Synergistic effects of brain death and liver steatosis on the hepatic microcirculation. Transplantation 2005;80(4):500–5. doi:10.1097/01.tp.0000167723.46580.78.
[32] Whalen WA, Berg CM. Gratuitous repression of avtA in Escherichia coli and Salmonella typhimurium. J Bacteriol 1984;158(2):571–4. doi:10.1128/jb.158.2.571-574.1984.
[33] Gall WE, Beebe K, Lawton KA, Adam KP, Mitchell MW, Nakhle PJ, et al. alpha-hydroxybutyrate is an early biomarker of insulin resistance and glucose intolerance in a nondiabetic population. PLoS ONE 2010;5(5):e10883. doi:10.1371/journal.pone.0010883.
[34] Faria J, Loureiro I, Santarém N, Cecílio P, Macedo-Ribeiro S, Tavares J, et al. Disclosing the essentiality of ribose-5-phosphate isomerase B in Trypanosomatids. Sci Rep 2016;6:26937. doi:10.1038/srep26937.
[35] Timson DJ. The molecular basis of galactosemia – past, present and future. Gene 2016;589(2):133–41. doi:10.1016/j.gene.2015.06.077.
[36] Memon N, Weinberger BI, Hegyi T, Aleksunes LM. Inherited disorders of bilirubin clearance. Pediatr Res 2016;79(3):378–86. doi:10.1038/pr.2015.247.
[37] Lattimer JM, Haub MD. Effects of dietary fiber and its components on metabolic health. Nutrients 2010;2(12):1266–89. doi:10.3390/nu2121266.
[38] Tvrzicka E, Kremmyda LS, Stankova B, Zak A. Fatty acids as biocompounds: their role in human metabolism, health and disease – a review. Part 1: classification, dietary sources and biological functions. Biomed Pap Med Fac Univ Palacky Olomouc Czech Repub 2011;155(2):117–30. doi:10.5507/bp.2011.038.